Russian Chemical Reviews **75** (6) 497 – 506 (2006) © 2006 Russian Academy of Sciences and Turpion Ltd

DOI 10.1070/RC2006v075n06ABEH003635

Nuclear magnetic resonance studies of translational diffusion in thermotropic liquid crystals

S V Dvinskikh, I Furó

Contents

I.	Introduction	497
II.	NMR methods for measuring diffusion in liquid crystals	498
III.	Theoretical models and computer simulations of diffusion in liquid crystals	500
IV.	Experimental studies of diffusion in thermotropic liquid crystals	501
V.	Conclusion	504

Abstract. The experimental NMR techniques for studies of translational diffusion in anisotropic systems and the results of their applications to thermotropic liquid crystals are reviewed. The main approaches to the theoretical description and computer simulations of diffusion are discussed. The experimental results are compared with computations. The bibliography includes 194 references.

I. Introduction

Liquid crystals (LC) represent substances that exist, under certain conditions, in a particular state that is intermediate between the solid and liquid states.

Liquid crystals or mesophases are formed by asymmetric rod-like or discotic molecules.[1] Depending on the method of preparation of LC, thermotropic and lyotropic systems are distinguished. The former result from thermal influence on mesogenic solid crystals, while the latter are formed upon dissolution of mesogenic molecules in certain solvents. Liquid-crystalline ordering stems from the anisotropic pair potential among mesogenic molecules. As a result of this interaction, molecules tend to align preferentially along the same spatial direction called a director. Quantitatively, this orientational order is characterised by the order parameter $S = 0.5\langle 3\cos^2\vartheta - 1\rangle$, where ϑ is the angle between the molecular symmetry axis and the director. Depending on the spatial arrangement of the mesogenic molecules, LC are subdivided into nematic, cholesteric, smectic and columnar phases.[1] Nematics exhibit one-dimensional orientational order. In smectic and columnar phases, in addition to the orientational order, a positional molecular order is present (molecules are arranged to form layered or column-like structures, respectively).

Molecules in liquid crystals exhibit high translational mobility. Combination of spatial ordering of the molecules with their high mobility opens the prospects for the practical applications of LC, which, in turn, stimulates the interest in fundamental studies of mesophases.[1–7]

In contrast to isotropic liquids where the self-diffusion is described by a scalar diffusion coefficient D, the translational self-diffusion in LC is characterised by a tensor $\mathbf{D}$.[8–11] In LC with the axial symmetry, two of the three principal components $D_{\alpha\alpha}$, $D_{\beta\beta}$, $D_{\gamma\gamma}$ of the diffusion tensor are equal in magnitude.[11,12] Conventionally, diffusion coefficients $D_\parallel$ and $D_\perp$ denote diffusion along and perpendicular to the director, respectively.

Diffusion in LC has been studied by a variety of experimental techniques including nuclear magnetic[8,9,11,13] and electron spin[14–16] resonances, quasielastic neutron scattering (QENS),[17–26] forced Rayleigh scattering,[27–35] optical microscopy[36–42] and radioactive tracer method.[43–45] NMR is currently the predominant method in diffusion studies of liquid crystals primarily because in most of the other techniques it is the diffusion of the molecular labels that is measured, which reflects only indirectly the diffusion of the molecular species in LC.

The past decade has witnessed significant advances in the NMR techniques. Novel procedures for the diffusion studies in LC have been developed;[46–60] that based on the magnetic pulsed field gradient spin-echo technique is unique because it is molecularly selective and requires neither foreign probes nor changing the LC properties.[61–67] Molecular positions and their changes are encoded by the NMR frequency, which becomes a function of the position in the presence of a magnetic field gradient.

The development of new techniques has allowed much more accurate measurements in a far broader range of diffusion coefficients. This has stimulated studies of 'difficult' and less conventional LC phases and determination of the diffusion tensor components in the phase transition region. With these new improved techniques it was also shown that some previous diffusion data were erroneous. New experimental results have motivated the development of new theoretical models and computer simulations of the diffusion process in liquid crystals.

In the present review, the experimental NMR techniques for diffusion studies in thermotropic liquid crystals are considered. The experimental results are compared with those derived from theoretical modelling and computation. The previous exhaustive review of diffusion studies in liquid crystals was published more than 20 years ago by Krüger[8] and was followed by brief recent surveys[9,10] and a methodological review.[11]

S V Dvinskikh Institute of Physics, St Petersburg State University, ul. Ul'yanovskaya 1, 198504 St Petersburg, Russian Federation. Fax (7-812) 428 72 40, tel. (7-812) 428 75 59, e-mail: sdvinskikh@mail.ru
I Furó Department of Chemistry, Royal Institute of Technology, Teknikringen 30/36, SE-10044 Stockholm, Sweden. Fax (46-8) 790 82 07, tel. (46-8) 790 85 92, e-mail: ifuro@physchem.kth.se

Received 17 March 2006
Uspekhi Khimii **75** (6) 557 – 568 (2006); translated by S V Dvinskikh

II. NMR methods for measuring diffusion in liquid crystals

In ordinary liquids, the NMR spectra consist of narrow lines because anisotropic spin interactions are all motionally averaged to zero due to rapid isotropic tumbling of the molecules. In contrast, in liquid crystals this local motional averaging is incomplete [3] and anisotropic spin couplings, such as the dipole–dipole or quadrupole interactions, are averaged to non-zero residual value. Hence, experimental NMR spectra usually exhibit line broadening and splitting. Spectral broadening translates into a quick decay of spin coherences in the time domain, which has a direct detrimental bearing on field-gradient NMR experiments for diffusion.

1. Pulsed-field-gradient NMR experiments

The determination of diffusion in conventional NMR experiments in isotropic liquids usually employs the pulse gradient spin echo (PGSE) [64–67] or the pulse gradient stimulated spin echo (PGSTE) † (Ref. 68) radio-frequency (rf) pulse sequences depicted in Fig. 1. Irrespective of the specific experiment, NMR detects displacement *via* gradient-assisted de- and re-phasing of spin coherences. Diffusion coefficients can be measured only if the spin coherences are sufficiently de-phased by the applied field gradient.

In isotropic liquids, the resulted spin echo amplitude is described by the well-known Stejskal–Tanner [62, 69] expression

$$A(g, \delta, \Delta) \sim \exp\left[-D\gamma^2 g^2 \delta^2 \left(\Delta - \frac{\delta}{3}\right)\right], \qquad (1)$$

where g and δ are the strength and the length of the applied gradient pulses, respectively, Δ is the diffusion time (the delay between gradient pulses), D is the self-diffusion coefficient and γ is the gyromagnetic ratio of the observed nuclei.‡ In anisotropic systems, this expression is modified to accommodate for the diffusion anisotropy [Eqn (2)]:[11, 69, 70]

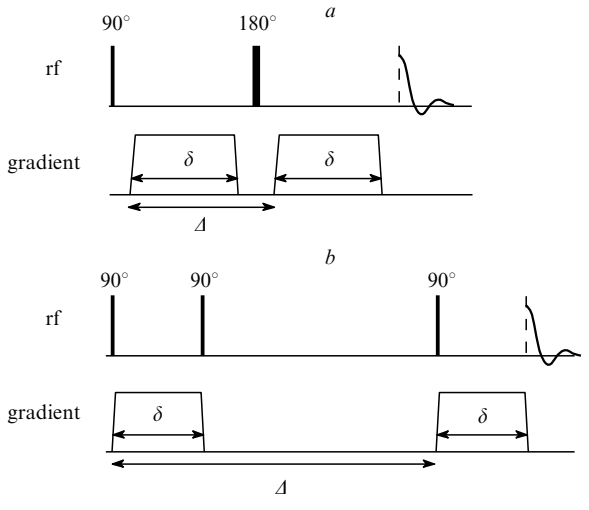


Figure 1. Pulse sequences for conventional pulsed-field-gradient spin echo (*a*) and stimulated echo (*b*) NMR experiments; δ is the length of the gradient pulses, Δ is the time delay between the gradient pulses.

$$A(\boldsymbol{g}, \delta, \Delta) \sim \exp\left[-\gamma^2 \delta^2 \left(\Delta - \frac{\delta}{3}\right) \boldsymbol{g}\boldsymbol{D}\boldsymbol{g}\right]. \qquad (2)$$

The quick decay due to relaxation processes sets an upper limit for the length of applicable gradient encoding/decoding pulses and, thereby, a lower limit for the measurable diffusion coefficients. Whether or not the line broadening can be suppressed depends on the dominant spin interaction and the magnitude of the residual coupling.

2. Spin interactions and the NMR spectral shape

The residual spin interactions depend on the orientation of local LC director with respect to the applied static magnetic field $\boldsymbol{B}_0$. If this orientation varies at short distances, spectral splitting by residual couplings may even vanish due to molecular reorientation induced by translational displacement. The director orientation with respect to the direction of the external magnetic field can be homogeneous or randomly distributed in the sample. Low-viscous LC can be prepared in a homogeneous state with the same director orientation all over the sample volume by applying suitable electromagnetic fields. For example, in many nematics the molecular axes orient spontaneously along the field vector in the magnetic field. This is a consequence of the positive anisotropy of the magnetic susceptibility $\Delta\chi = \chi_{\parallel} - \chi_{\perp}$ of molecules ($\chi_{\parallel}$ and $\chi_{\perp}$ are susceptibilities parallel and perpendicular to the director, respectively). The contribution to the free energy

$$\Delta G = -\frac{1}{6}\Delta\chi B_0^2 (3\cos^2\vartheta - 1)$$

(ϑ is the angle between the director and the field vector) due to coupling to a magnetic field B_0 is minimised for the director alignment parallel to the field. Although $\Delta\chi$ is relatively small, the collective effect in the bulk sample is sufficient to overcome thermal fluctuations. Such oriented systems are contrasted to 'powder' samples with the random angular orientation of the director.

The appearance of the spectrum also depends on the involved spin couplings. The pairwise dipole–dipole interactions usually act in LC among a manifold of nuclei. Hence, even in uniformly oriented LC samples [*e.g.*, in 4-cyano-4′-pentylbiphenyl (5CB)] ^{1}H NMR spectra of dipole–dipole coupled ^{1}H nuclei are wide because they consist of many overlapping split lines (Fig. 2).

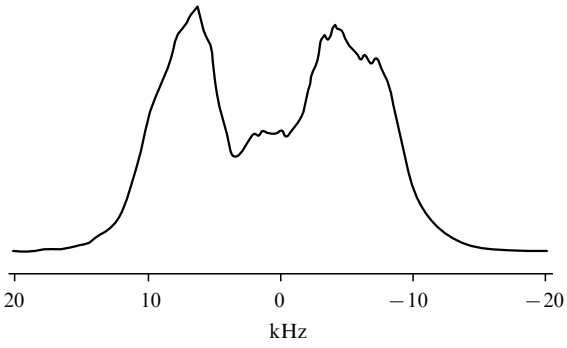


Figure 2. ^{1}H NMR spectrum of nematic 4-cyano-4′-pentylbiphenyl (5CB).

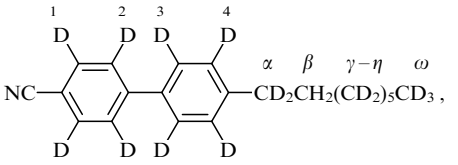
The exception is LC where the director of a sample is oriented at the 'magic angle' ϑ_m to $\boldsymbol{B}_0$, since at this condition the splitting and the resulting spectral broadening are suppressed.§ Single-spin quadrupole interactions for spin $I = 1$ nuclei in a macroscopically

† In the absence of motion, all de-phased magnetisation can be recovered in the form of echo signal.[68]

‡ Since dephasing is proportional to γ^2, the majority of NMR diffusion measurements have been carried out on high-γ nuclei, mainly ^{1}H.

§ At $\vartheta_m = \text{acos}(1/\sqrt{3}) \approx 54.7°$ (ϑ_m), the angular factor in the dipole–dipole interaction term is equal to zero; hence, the corresponding contribution to the spectral line width vanishes.

oriented LC may result in spectra split into sharp lines. For example, the ^{2}H NMR spectrum of partially deuterated 4-cyano-4′-octylbiphenyl (8CB)



consists of quadrupolar split doublets (Fig 3).

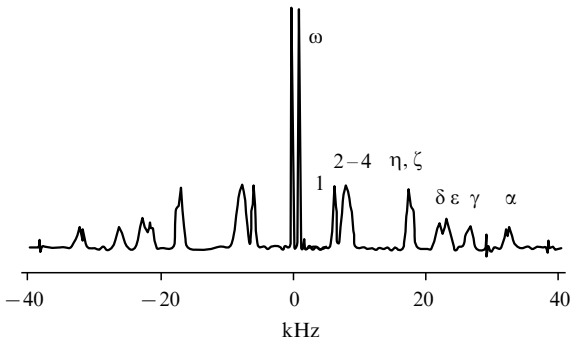


Figure 3. ^{2}H NMR spectrum of partially deuterated smectic 4-cyano-4′-octylbiphenyl (8CB).

Powder samples exhibit, irrespective of the type of the involved spin interaction (dipole–dipole and quadrupolar), large broadening but often, for the latter case, with a discernible 'powder pattern' line shape with the characteristic singularities.[71]

3. Measurement of diffusion coefficients in liquid crystals

Diffusion in thermotropic liquid crystals has been addressed by a broad range of NMR techniques,[8,9,11] including static-field-gradient method,[47,59,60] as well as various techniques combining pulsed field gradients with a 'nematic' echo sequence,[72–74] multiple-pulse spin decoupling,[11,49–55,75–77] magic-angle sample orientation,[46,56–58,73,78–82] deuterium stimulated (alignment) echo,[53] soft-pulse excitation[83] and multiple-quantum NMR.[55,84,85] The optimum choice depends on the type of spin interaction, spectral shape and macroscopic sample orientation. Thus, conventional PGSE and PGSTE techniques have been used for weakly oriented solutes in liquid crystalline matrices.[3,8,86–88]

a. Sample alignment at the magic angle

The simplest and earliest method for the diffusion coefficient measurement involves the preparation of a homogeneously oriented sample, which is then placed by its director at the magic angle (54.7°) with respect to the magnetic field $\boldsymbol{B}_0$.[79] In LC with the uniaxial symmetry of the orientational order, this rotation suppresses the dipole-dipole broadening. The limitation of the method is the required uniform orientation at a given oblique angle to the magnetic field; hence, this technique is not available in liquid-crystalline phases that reorient in the magnetic field or cannot be uniformly oriented. Hence, this approach has mainly been used for studies of viscous smectic phases formed upon cooling of nematic phases.¶ For nematic phases, the electric field has been employed to hold the director along the magic angle.[78]

In yet another approach, fast switching of the B_0 direction in a field-cycling spectrometer[46] creates the magic-angle condition. A late offspring of magic-angle technique, appropriate for studies of unoriented powder-like LC samples, is a diffusion experiment performed under magic angle spinning (MAS) conditions[89] with the gradient field set along the spinning axis.

b. Suppression of anisotropic spin interactions by echo techniques

In the case of small anisotropic dipole–dipole ($I = 1/2$) or quadrupole couplings ($I = 1$), one may apply the solid or quadrupole echo[90,91] instead of a conventional spin echo. In some cases, the so-called nematic echo[92,93] generated in a $90°-\tau-\beta-\tau$ sequence with $\beta < 54.7°$ has been observed in ^{1}H NMR and employed in diffusion experiment.[73,74,94] For ^{2}H NMR experiments, the stimulated echo sequence with modified pulse flip angles has been suggested to suppress the effect of the quadrupolar coupling on the echo amplitude.[53]

c. Spin decoupling

Line broadening effects for systems of nuclei with $I = 1/2$ are in most cases significant due to homonuclear dipolar interactions. In solids, static dipolar line broadening is usually suppressed by appropriate radio frequency pulse sequences.[95] The same strategy has been explored for anisotropic diffusion experiments. The problem is that dipolar decoupling sequences perform inefficiently in the presence of a large frequency offset induced by the applied field gradient.[96] Hence, initially only very short (and, hence, weak due to instrumental limitations) gradient pulses in-between the rf pulses of the homonuclear decoupling sequence have been applied.[75,76] As a consequence, only relatively fast diffusion could be measured this way. A better choice is to apply magic-echo (Fig. 4)[53,97] decoupling during evolution periods of the stimulated echo pulse sequence.[98] In this sequence, longer windows are available for gradient pulses. Magic echo, originally devised to remove multi-spin dipole–dipole coupling, has also been shown to suppress simultaneously static quadrupole effects.[99] Hence, this strategy has been applied to quadrupolar spins with non-vanishing dipolar couplings.[53–55] The disadvantage of the experiment is the limited time available for gradient encoding: at most, one-third of the coherence evolution periods.

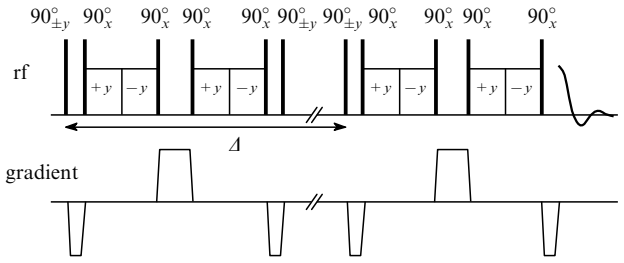


Figure 4. Stimulated echo sequence combined with magic-echo decoupling for measuring diffusion coefficients in the presence of static dipole–dipole and/or quadrupole interactions in LC.[53]

Decoupling in the presence of uninterrupted gradient pulses[100,101] is more effective. However such experiments can only be made accurate if the resonance frequency offset effects of decoupling are correctly dealt with. This can be achieved using slice selection by a soft 180° pulse (Fig. 5), which limits the active sample volume to the region with sufficiently small frequency offset.[49–51] Applied to homonuclei,[49,51] this strategy suffers from two shortcomings: down-scaling of the gradient by the decoupling sequence, which limits the efficiency of gradient encoding and a decrease in the signal intensity as a result of slice selection. In the case of heteronuclei,[50] there is no down-scaling of gradient and the slice selection scheme can be 'multiplexed' thereby collecting the signal from most of the sample volume.

¶ Once oriented by the magnetic field in the nematic phase and subsequently transformed upon cooling to the smectic state, many samples preserve a homogeneous director orientation even when turned away from $\boldsymbol{B}_0$.

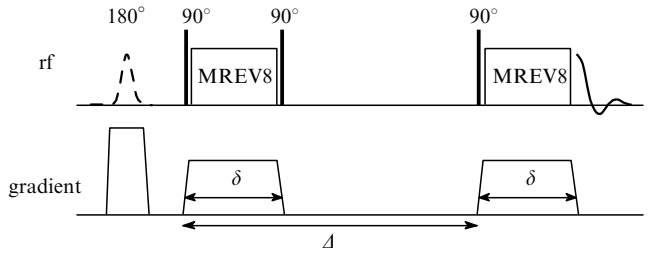


Figure 5. Pulse sequence for diffusion measurements using stimulated echo experiment with homonuclear decoupling (by MREV8 sequence)[95] applied simultaneously with the field-gradient pulses.[49]

d. Multiple-quantum NMR

An additional possibility, explored not only in the case of $I = 1$ nuclei,[54] but also in the situation of dipolar coupled spins $I = 1/2$,[84,85] is to perform an experiment where gradient pulses are employed during the evolution of multiple-quantum spin coherences. The highest-order coherences are not influenced by static quadrupolar and dipolar effects and, hence, exhibit longer decay.[102] As an additional advantage, the field gradient affects higher-quantum coherences proportional to their quantum order thereby increasing the efficiency of gradient encoding/decoding.

e. Strong field gradient

Instead of suppressing line broadening, one may try a 'brute force' approach, *viz*., to increase the strength of the gradient field. One way is to use a small gradient coil in combination with a high-current generator.[103–111] The other solution is to exploit static gradients such as the one present in the fringe field of a conventional NMR superconducting magnet.[112,113] The rf pulse sequence in this case is similar to that shown in Fig. 1 *b*, but with the gradient field constantly present instead of the pulsed gradient.[47,59,60,114] An obvious disadvantage is small signal-to-noise ratio, which is a consequence of the limited range of excitation of the applied rf pulses and of the spectral broadening by the gradient during detection. Moreover, one cannot conveniently vary the gradient strength and direction.

f. Spectral selective excitation

Spatial slice selection can be replaced by spectral slice selection by long selective rf pulses.[83] It has been shown that weak rf pulses can excite sharp proton signals in ^{1}H NMR spectra of liquid crystals,[115] which can be exploited for measurements of their diffusion coefficients.[83] Just as for spatial slice selection, the signal loss is a disadvantage of this approach.

g. Relaxation

Diffusion coefficients can be estimated from the NMR spin relaxation rate measurements.[116–123] An access to diffusion *via* relaxation, however, requires the separation of contributions to the relaxation rates of intra- and intermolecular interactions as well as contributions of different modes of molecular reorientations. The contribution of the intermolecular interaction to spin relaxation processes originates from the modulation of dipole–dipole interactions upon molecular diffusion.[124–127] Diffusion coefficients extracted from the relaxation data characterise the translational motion on the molecular length-scale in contrast to the micrometre-scale diffusion coefficients obtained by the field-gradient techniques.

h. Spectral shape analysis

Chiral mesophases (cholesterics) exhibit helical spatial modulation of the molecular orientation. If the NMR spectral shape is dominated by the anisotropic spin interactions, the resonance frequency turns out to be spatially encoded even without the application of an external field gradient.[128–137] Modulation of the spin resonance frequency as a result of molecular diffusion is reflected in the shape of the NMR spectrum, akin to chemical exchange effects.[138] Note, this approach can only measure the diffusion component along the modulation direction, *i.e*., along the helical axis.

4. Accessing the diffusion tensor components

Characterisation of the diffusion tensor $\boldsymbol{D}$ requires experiments performed at several field gradient orientations with respect to the director. In a homogeneously oriented sample, $D_\parallel$ and $D_\perp$ can be measured either by using orthogonal gradient coils[52,53,55,57,58,139] or by changing the sample orientation provided that the director is not re-oriented by the magnetic field.[46,60,78,82] The other option, applicable in non-oriented samples, exploits the spectral broadening itself by anisotropic spin interactions, such as quadrupole coupling[90] or chemical shift anisotropy.[51,140] Since the anisotropic interactions provide correspondence between the spectral resonance frequency and the domain orientation, the intensity decay at different frequencies in the spectrum for just one gradient direction reveals the principal components of the diffusion tensor $\boldsymbol{D}$.

If diffusion within individual domains of non-oriented powder samples cannot be orientationally assigned (as is typical of the ^{1}H nuclei), the diffusional decay becomes the composite of decays for different gradient orientations.[11,141] If the orientational distribution is completely random and other effects, such as restricted diffusion, do not complicate the evaluation, the diffusion tensor can also be extracted either from the composite decay or from diffusion–diffusion correlation (or exchange) experiments using orthogonal field gradient pulses.[142–144]

III. Theoretical models and computer simulations of diffusion in liquid crystals

1. Diffusion models in nematics

Several theoretical approaches have been developed to describe the translational diffusion in nematic liquid crystals. The hydrodynamic theory of Franklin[145] evaluates the molecular diffusion in terms of viscosity coefficients, friction constants and detailed molecular geometry. Using this approach, the temperature dependence of the anisotropic radio-tracer diffusion in the nematic phase of *p*-azoxyanisole (PAA) was correctly predicted.[145] In contrast, the results obtained for nematic 5CB were found to be incompatible with this model.[52,55] Since the approach involves many parameters not readily available with sufficient accuracy, its predictions cannot be easily verified by experiments.

In yet another approach, the diffusion coefficients in nematic phases have been derived *via* a parameterised form of the momentum time-autocorrelation function in the system of perfectly ordered clusters and subsequent transformation of the diffusion tensor from the cluster frame to the laboratory frame.[146] The theory relates the components of the diffusion tensor to the molecular geometry (molecular axial ratio) and the order parameter S. It predicts that the arithmetic (isotropic) average of the diffusion coefficient

$$\langle D\rangle_{\mathrm{a}} = \frac{2D_\perp + D_\parallel}{3} \tag{3}$$

is independent of orientational order and geometry and changes continuously across the nematic–isotropic phase transition. The model has previously been applied with varying success to nematic liquid crystals. Particularly, a satisfactory agreement with the results in PAA was found.[146]

Hess and co-workers[147] have applied the affine transformation from the isotropic diffusion of hard spheres to the space of aligned uniaxial ellipsoids to derive the diffusion coefficients in terms of the molecular axial ratio and the phase order parameter. In contrast to the previous approach, the geometric average

$$\langle D\rangle_{\mathrm{g}} = D_\parallel^{1/3} D_\perp^{2/3} \tag{4}$$

rather than the isotropic average $\langle D\rangle_g$ is predicted to be independent of the molecular shape and order and to coincide at the phase boundary with the diffusion coefficient in isotropic phase. This model has been successfully tested using molecular dynamics computer simulations [147, 148] and describes well experimental NMR results.[52, 53]

A mean-field kinetic approach to anisotropic translational diffusion in nematics has also been proposed.[149] Similarly to the affine transformation model, the predicted value of $\langle D\rangle_a$ increases with the increase in the molecular order.

2. Diffusion models in smectics

The diffusion in the smectic A phase has been modelled under the assumption of a periodic temperature-independent potential $V(z)$ along the smectic director [150–152]

$$V(z) = \frac{V_1}{2}\cos\left(\frac{2\pi z}{d}\right), \tag{5}$$

where d is the layer spacing. Thus, diffusion parallel to the director requires the molecule to overcome not only the viscous drag of the medium, but also the potential barrier. In-layer diffusion remains essentially unaffected. Molecular diffusion along the director is given by the equation

$$(D_\parallel)^{sm} = (D_\parallel)^{nem}\left[I_0\left(\frac{V_1}{2RT}\right)\right]^{-2}, \tag{6}$$

where I_0 is the modified Bessel function of the first kind and of the zero order. For the non-zero potential amplitude, V_1, this model predicts a discontinuity of $D_\parallel$ at the nematic–smectic A phase transition. This approach has successfully described diffusion data obtained by QENS and NMR methods in some smectic LC with a pronounced discontinuity of $D_\parallel$ at the nematic–smectic phase transition.[8, 94]

Recently,[55] this model has been modified to include a temperature-dependent potential in the parameterised form:

$$V_1(T) = V_0\left(1 - \frac{T}{T^*}\right)^\gamma \tag{7}$$

in keeping with the temperature dependence of McMillan's smectic order parameter.[153] The value of the parameter T^* is close to the smectic–nematic transition temperature. This modified model provided a correct description of the experimental results in smectic A phases with a weak second order nematic–smectic phase transition as is typical of systems exhibiting a significant nematic range.[55, 80, 81]

3. The temperature dependence of the diffusion coefficients

Arrhenius-type descriptions are commonly applied to the temperature dependence of the individual components of the diffusion tensor in liquid crystals,[8, 9]

$$D_{\parallel,\perp} = D^0_{\parallel,\perp}\exp\left(-\frac{E_{\parallel,\perp}}{RT}\right). \tag{8}$$

However, the energy parameter E does not have a simple physical meaning in the case of liquid crystals, in contrast to solids where it corresponds to the height of the potential barrier for particle jumping between the lattice sites. The values $E_{\parallel,\perp}$ in mesophases may be dependent on the temperature through the order parameter, especially near the phase transitions.[52] Thus, although Eqn (8) has often been found to fit well the experimental data recorded in mesophase temperature ranges, the numerical results lack physical interpretation.

4. Computer simulation of the diffusion by molecular dynamics

In molecular dynamics (MD) simulation of diffusion in liquid crystals,[148, 149, 154–164] the diffusion coefficients were determined either from the mean-square molecular displacements or from the velocity autocorrelation functions. The results are commonly compared to those predicted based on the affine transformation model and to experimental data.

A non-monotonic temperature dependence of $D_\parallel$ in nematic phase was observed,[148, 164] which was attributed to the competition between a decrease in molecular ordering and mobility. The geometric average of the diffusion coefficient $\langle D\rangle_g$ was found to be continuous and linearly temperature-dependent across the nematic–isotropic phase transition. In contrast, the isotropic average $\langle D\rangle_a$ depends on molecular order,[164] as illustrated in Fig. 6.[163, 164]

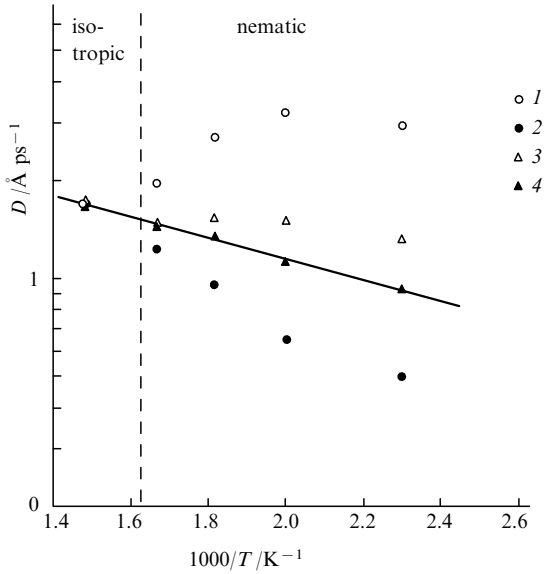


Figure 6. The temperature dependences of the diffusion tensor components and their averages as obtained from MD simulation.[164] (*1*) $D_\parallel$, (*2*) $D_\perp$, (*3*) $\langle D\rangle_a$, (*4*) $\langle D\rangle_g$.

Calculations of mean-square displacements were performed in a system of soft-core spherocylinders (cylinders with hemispherical caps) interacting by an inverse-power pair potential.[154] The obtained data showed that, in the smectic A phase, diffusion takes place exclusively along the layer. In an MD simulation of a Gay-Berne mesogen,[163] $D_\parallel$ was shown to change abruptly for the phase sequence isotropic–smectic A, which is characteristic of a first-order phase transition, and $D_\parallel < D_\perp$. However, if the system also exhibits an extended nematic phase, starting from $D_\parallel(\text{smec A}) \approx D_\parallel(\text{nem})$ in the vicinity of nematic–smectic A transition, the $D_\parallel > D_\perp$ nematic property permeates the smectic A phase and may become inverted at lower temperatures. The coefficient $D_\perp$ essentially follows the same temperature trend well described by the Arrhenius law over the whole range of smectic and nematic phases. This type of diffusion was observed experimentally in liquid crystals of 8CB.[55]

MD simulation has been performed in the columnar phase of the discotic molecules of hexakis(pentyloxy)triphenylene.[165] The diffusion process exhibited a solid-like jump behaviour in the plane perpendicular to the columnar axis. The translational dynamics of the molecules along the axis was described by the model of column sliding.

IV. Experimental studies of diffusion in thermotropic liquid crystals

Early NMR diffusion experiments in thermotropic nematic [8, 72, 74, 75, 77, 88, 166] and smectic systems [8, 73, 76, 79, 80] often merely recorded the fact that the diffusion is anisotropic. The experimental accuracy, reproducibility and the range toward slow diffusion were limited, as has been demonstrated recently

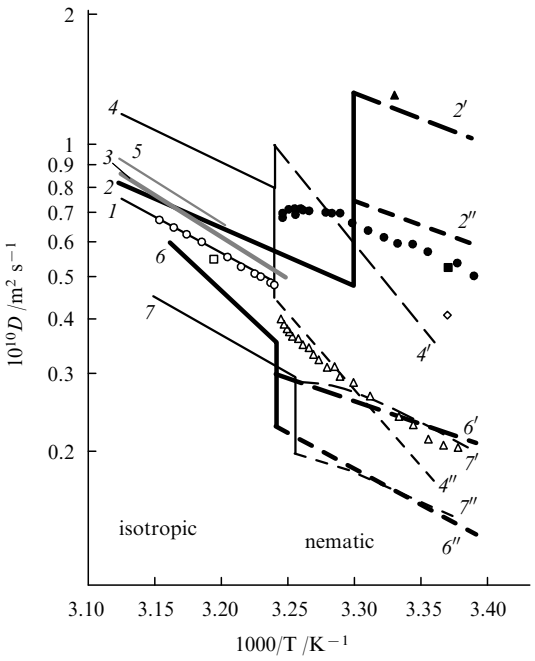


Figure 7. Data on anisotropic diffusion in 5CB as obtained by spin-decoupling-based NMR diffusion experiments (○ — D_{iso}, ● — $D_{\|}$, △ — $D_{\perp}$),[52] in comparison with the results obtained by other techniques: PGSE NMR (*1*) D_{iso},[167] [(*2*) D_{iso}, (*2′*) $D_{\|}$, (*2″*) $D_{\perp}$];[168] fringe-field NMR (*3*) D_{iso};[169] field cycling NMR [(*4*) D_{iso}, (*4′*) $D_{\|}$, (*4*)″ $D_{\perp}$];[46] PGSE NMR with the sample reorienting in the electric field [(*5*) D_{iso}, ▲ — $D_{\|}$];[78] forced rayleigh scattering [(*6*) D_{iso}, (*6′*) $D_{\|}$, (*6*)″ $D_{\perp}$],[27] [(*7*) D_{iso}, (*7′*) $D_{\|}$, (*7″*) $D_{\perp}$];[35] QENS (□ — D_{iso}, ■ — $D_{\|}$, ◇ — $D_{\perp}$).[19]

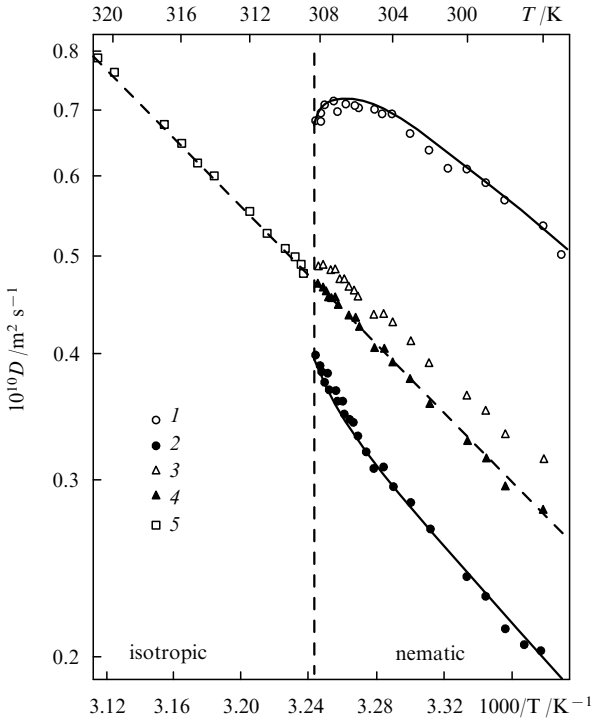


Figure 8. Values of $D_{\|}$ (*1*), $D_{\perp}$ (*2*), $\langle D\rangle_a$ (*3*), $\langle D\rangle_g$ (*4*) and D_{iso} (*5*) in 5CB obtained by multiple-pulse spin-decoupling-based NMR experiment.[52] Solid lines are the fits by the affine transformation model.[147]

(Fig. 7).[52] The early works performed up to 1982 have been comprehensively reviewed by Krüger,[8] and hence are only briefly recalled here.

A parameter that can be measured with the acceptable accuracy is the activation energy, since it may be obtained from the strong temperature dependence of the diffusion coefficient. The values of the activation energies $E_{a\|} \approx E_{a\perp}$ that have been obtained in nematic liquid crystals were comparable to those in isotropic phases. In smectics, the relationships $E_{a\|} > E_{a\perp}$ and $E_{a\perp}(\text{smec}) \approx E_{a\perp}(\text{nem})$ have generally been observed, which is consistent with the model of in-layer continuous diffusion in liquids and a jump process between the layers typical of solids.

The diffusion anisotropy $D_{\|}/D_{\perp}$ in nematic phase ranges between 1.2 and 4. Within the experimental accuracy, the values of the majority of average diffusion coefficients $\langle D\rangle_a$ in the nematic phase at the clearing point determined earlier were close to the isotropic diffusion coefficients. The ratio $D_{\|}/D_{\perp}$ in smectics was found to vary in a wider range from $D_{\|}/D_{\perp} \geqslant 1$ to $D_{\|}/D_{\perp} \ll 1$.

1. Diffusion in nematic and cholesteric phases

Nematic phases were frequently chosen for testing new techniques for the determination of diffusion coefficients in liquid crystals, the nematic phase of 5CB being the most popular model compound. Recently, the diffusion coefficients in 5CB obtained by different methods have been compared (see Fig. 7).[52] While earlier results strongly disagree, obviously due to methodological problems, more recent studies by advanced NMR techniques, including multiple-pulse-decoupling PGSTE,[52,55] fringe-field-gradient stimulated echo [47] and spectral-slice-selection PGSTE [83] demonstrate a good agreement.

The most accurate values of the diffusion tensor components in 5CB over a wide temperature range (Fig. 8) have been obtained by multiple-pulse-decoupling PGSTE NMR.[52,55] The temperature dependence of the diffusion coefficient D_{iso} in the isotropic phase is described with high accuracy by the Arrhenius equation. Although the temperature dependence of both $D_{\|}$ and $D_{\perp}$ in the nematic phase at the points far from the nematic–isotropic phase transition can be approximated by the Arrhenius-type relationship (with the activation energies $E_{a\|} < E_{a(iso)} < E_{a\perp}$), the two curves $D_{\|}(T)$ and $D_{\perp}(T)$ converge fast toward the isotropic value closer to the phase transition. This suggests that the anisotropy of the translational diffusion reflects the orientational ordering of the molecules, which decreases sharply on approaching the isotropic phase. The temperature dependence of the isotropic average $\langle D\rangle_a$ [see Eqn (3)] also deviates from the simple Arrhenius relationship in the vicinity of the phase transition. At the phase transition, there is an appreciable discontinuity between D_{iso} and $\langle D\rangle_a$. This behaviour contradicts that predicted from a model of a momentum time-autocorrelation function used for the diffusion coefficient calculations.[146] In contrast, calculations using the affine transformation model [147] are consistent with experimental results. In particular, the values of the geometric average $\langle D\rangle_g$ [see Eqn (4)] are on the line extrapolated from the isotropic phase. An analogous behaviour was observed in the nematic phases of 8CB (Refs 53, 55) and *N*-(4-ethoxybenzylidene)-4′-butylaniline (EBBA) [55] where the same types of multiple pulse techniques were employed.

Diffusion measurements have been performed in 4-(n-octyloxy)-4′-cyanobiphenyl (8OCB) and 4,4′-di-(n-octyl)azoxybenzene (OAB) using fringe-field-gradient NMR.[59,60] The temperature dependences of $D_{\|}$ in the nematic phase and at the isotropic–nematic phase transition resemble that in 5CB and 8CB. Since the temperature dependences of the $D_{\perp}$ component of the diffusion tensor were not measured and since the nematic phase in OAB exists in a limited temperature range, no comparison with the theoretical models was performed.

The temperature dependences of the principal components of the diffusion tensor were reported for homologous series of di(alkyl)azoxybenzenes and (alkoxy)cyanobiphenyls [46,82] using the field-cycling technique. A characteristic alternation of diffusion coefficients and activation energies as functions of the chain

length, *i.e.*, the familiar odd-even effect, has been observed. Unexpectedly, it was found [82] that both $D_{\parallel}$ and $D_{\perp}$ were larger than D_{iso}, which is probably due to systematic errors caused by methodological problems.

An anomalous temperature dependence † of the components of the diffusion tensor was also found in nematic 4-pentylphenyl 2-chloro-4-(4-pentylbenzoyloxy)benzoate.[100] This behaviour is most probably an artefact due to interference between the heteronuclear decoupling and the field gradient as discussed in Ref. 50.

Conventional PGSTE NMR has been applied for studying the diffusion behaviour in a cholesteric phase formed by 5CB doped with an optically active chiral component, *viz.*, 4-cyano-4′-(2-methyl)butylbiphenyl (CB15).[168] The orientation of molecules in a cholesteric phase corresponds to that in the nematic phase with the director helically twisted in space. The pitch axis of the twisted structure is aligned perpendicular to the direction of the magnetic field of a spectrometer. This experiment demonstrates the existence of the translational diffusion anisotropy (ratio $D_{\parallel}/D_{\perp} \approx 1.7$) with the diffusion coefficients dependent on the diffusion time.

In a number of diffusion studies in cholesteric phases, NMR spectral shape analysis has been used, which allowed measurement of only $D_{\perp}$, *i.e.*, diffusion along the pitch axis. It was shown that $D_{\perp}$ increases with pitch length and depends on the diffusion time.[128–130] The Arrhenius-type temperature dependence was commonly observed with apparent activation energies close to those in nematic phases and with relationship $D_{\perp} < D_{iso}$ at the clearing temperature (Fig. 9).[128, 131]

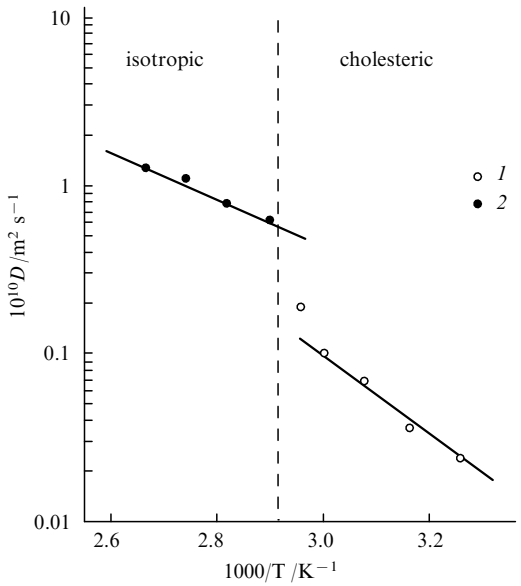


Figure 9. The temperature dependence of the diffusion coefficients in the isotropic and cholesteric phases of a mixture of substituted phenylbenzoates and chiral dopants.[131]
(*1*) $D_{\perp}$, (*2*) D_{iso}.

While diffusion coefficients in the isotropic phases of liquid-crystalline compounds commonly display simple Arrhenius-type temperature dependences,[47, 52, 55, 167, 169–174] accurate measurements performed in the vicinity of the isotropic–nematic phase transition on the isotropic side indicated a noticeable deviation from this conventional behaviour.[106, 175] This effect has been attributed to the formation of locally ordered nematic clusters (cybotactic groups) in isotropic surroundings.

† The experimental values of the activation energies in this nematics were related as $E_{\parallel} > E_{\perp}$, which is not typical of nematics.

2. Smectic phases

Smectics A exhibit high molecular mobility within the layers comparable to that in conventional liquids. Diffusion anisotropy in smectics typically becomes $D_{\parallel}/D_{\perp} < 1$,[8, 57, 76, 79] as opposed to that in nematics. At the nematic–smectic phase transition, $D_{\perp}$ changes nearly continuously, while $D_{\parallel}$ and its apparent activation energy change abruptly as a result of molecular jumps between adjacent smectic layers.[8, 55, 60] However, smectic A materials that exhibit a broad temperature range of the nematic phase display a different behaviour (Fig. 10): for them, the nematic-like relationship $D_{\parallel}/D_{\perp} > 1$ is typically found in the vicinity of the phase transition point.[55, 56, 58, 59, 81] Upon cooling deeper into the smectic phase, the diffusion ratio may change to the opposite, more common for smectics.[59, 73] As concerning the activation energies, the relation $E_{\parallel} \geqslant E_{\perp}$ is always fulfilled.

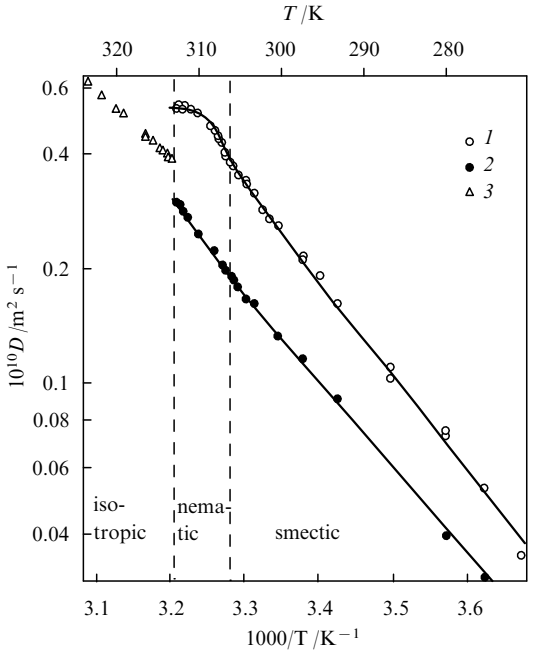


Figure 10. The temperature dependences of the diffusion coefficients in isotropic, nematic and smectic A phases of 8CB.[55]
Lines are fits by the affine transformation model [147] in the nematic phase and by a model with a temperature-dependent periodic potential in the smectic A phase.[55, 150]
(*1*) $D_{\parallel}$, (*2*) $D_{\perp}$, (*3*) D_{iso}.

Fringe-field-gradient stimulated echo has been applied [114] to measure the diffusion coefficients in different smectic A, C* and C_A^* phases ‡ of the liquid crystal of 1-methylheptyl 4′-[4-(n-decyloxy)benzoyloxy]biphenyl-4-carboxylate. A continuous decrease in the diffusion coefficient in the direction of the layer normal was observed in smectic A and C* phases, while an abrupt decrease by nearly two orders of magnitude was found on the transition to C_A^* phase. Similarly, slow interlayer diffusion in smectic C_A^* phase compared to phase C* has been detected using ^{2}H NMR spectral shape analysis.[137, 176] This finding was explained by steric effects arising from the anticlinal molecular arrangement in adjacent layers, which hinder the interlayer diffusion.

Experimental results obtained in smectic A phases [55, 59, 60] have been compared to the available theoretical models. Some results [59] were consistent with the model developed by Volino *et al.*,[150, 151] which predicts an abrupt decrease in $D_{\parallel}$ at the transition from nematic or isotropic phases to smectic A phases (Fig. 11).

‡ C* and C_A^* are chiral smectic phases C with synclinically and anticlinically ordered molecules, respectively.

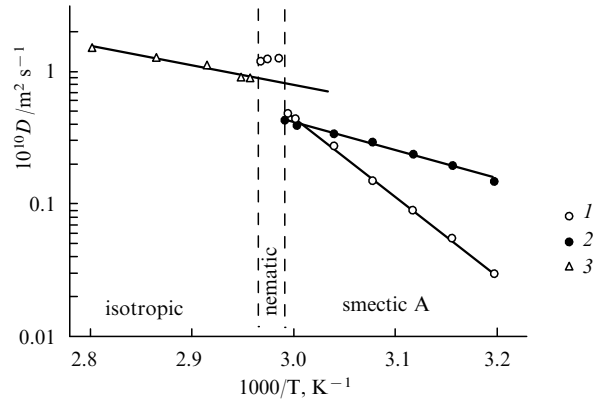


Figure 11. Diffusion coefficients of OAB obtained in the isotropic, nematic and smectic A phases.[59]
(*1*) $D_{\|}$, (*2*) $D_{\perp}$, (*3*) $D_{\rm iso}$.

However, for systems with a weak second-order nematic-to-smectic phase transition, a model with the temperature-dependent potential (see Eqn 7 and Fig. 10) should be assumed for the analysis of the experimental data. The behaviour of 8CB [55] and 8OCB [60] was correctly described in that way.

3. Columnar phases of discotic molecules

In contrast to conventional thermotropics built by rod-like mesogenic units, columnar phases are formed by discotic flat molecules.[177] For the columnar hexagonal phase of a discotic thermotropic hexapentyloxytriphenylene, it was shown that the diffusion is very slow [54] in contrast to early indications.[178] The diffusion in the direction perpendicular to the columnar axes was measured by ^{2}H PGSTE NMR. A low magnitude of the diffusion coefficient [$D_{\perp} = (1-4)\times 10^{-14}$ m^2 s^{-1}] and a high activation energy ($E_{\perp} = 115$ kJ mol^{-1}) suggested solid-like or, perhaps, collective diffusion mechanisms in discotics.[54]

4. Polymeric liquid crystals

Anisotropic diffusion with the relationship $D_{\|} > D_{\perp}$ relative to the α-helical chain axis and with apparent activation energies dependent on the main-chain length has been observed in LC phases formed by rod-like polypeptides.[179–181] In the polymeric LC phase formed by flexible poly(diethysiloxane) molecules, the diffusion was found to be faster than that in the isotropic phase.[182] This was attributed to a decrease in the degree of entanglement between the polymer chains that become orientationally correlated in the anisotropic phase.[182]

5. Liquid crystals confined in porous media

The effect of confinement on the diffusion properties of LC embedded in porous glass matrices (with the pore size varied from 7.5 to 140 nm) was studied for the nematic 5CB as an example.[47] A strong decrease in the diffusion coefficient with the decrease in the pore size was observed. The PGSE NMR measurement of self-diffusion in nematic EBBA confined in porous glasses was used to estimate the size of the nematic clusters in the isotropic pre-transition region adjacent to the nematic phase.[106]

6. Diffusion of small solute molecules in mesophases

Due to their low orientational order, small organic molecules dissolved in liquid crystals exhibit long decays of spin coherences. Therefore, conventional PSGE or PGSTE experiments can be used to assess their diffusion coefficients.[8, 14, 72, 86, 87, 183–189] In nematic phases, the solute diffusion is fast and the diffusion anisotropy is small, as compared to the diffusion of molecules forming a mesophase.[8, 9] This contrasts the strong translational diffusion anisotropy $D_{\|}/D_{\perp} \ll 1$ observed in smectic phases.[8]

Recently, the diffusional behaviour of xenon in liquid crystals has been studied in detail.[190–194] PGSE ^{129}Xe NMR has been used to probe diffusion of xenon dissolved in nematic [190, 191, 194] and smectic (A and C*) phases.[192–194] No diffusion anisotropy and very weak anisotropy ($D_{\|}/D_{\perp} > 1$) were observed in the nematic phases of ZLI-1132 [190] and EBBA/ZLI-1167,[191] respectively. In contrast, significant anisotropy was found in smectic phases of ferroelectric liquid crystals, where $D_{\|}/D_{\perp} \ll 1$.[192, 193]

V. Conclusion

A number of new diffusion techniques applicable to liquid crystals have been developed during the past decade. In contrast to techniques applied for isotropic liquids, these advanced approaches with various degrees of sophistication have not yet become routine tools. However, when applied with insight, the new techniques provide much higher accuracy and significantly extend the range of the accessible diffusion coefficients.

Self-diffusion data provide detailed and easily interpreted information on the molecular organisation and dynamics in mesophases. The anisotropic diffusion tensor and the activation energy in liquid crystals are very sensitive to structural changes at the phase transitions. Observing the changes in components of the diffusion tensor at the phase transitions allow a thorough evaluation of, and discrimination among, the theoretical models as well as the assessment of the computer simulation data. For conventional thermotropic phases, such as nematics and smectics A, the accurate diffusion data obtained with advanced NMR methods are well understood in terms of available theoretical models. For other systems, including highly ordered columnar and smectic phases generally exhibiting slow diffusion, only limited data are available as yet.

This work was supported by the Russian Foundation for Basic Research (Project Nos 04-03-32639 and 05-08-50280) and by the Swedish Research Council VR.

References

1. D Demus, J W Goodby, G W Gray, H-W Spiess, V Vill *Handbook of Liquid Crystals* (Weinheim: Wiley-VCH, 1998)
2. P-G de Gennes *The Physics of Liquid Crystals* (Oxford: Clarendon, 1974)
3. R Y Dong *Nuclear Magnetic Resonance of Liquid Crystals* (New York: Springer, 1994)
4. G R Luckhurst *Liq. Cryst.* **32** 1335 (2005)
5. E E Burnell, C A de Lange (Eds) *NMR of Ordered Liquids* (Dordrecht: Kluwer Academic, 2003)
6. A S Sonin *Vvedenie v Fiziku Zhidkikh Kristallov* (Introduction to Physics of Liquid Crystals) (Moscow: Nauka, 1983)
7. S A Pikin, L M Blinov *Zhidkie Kristally* (Liquid Crystals) (Moscow: Nauka, 1982)
8. G J Krüger *Phys. Rep.* **82** 229 (1982)
9. F Noack, in *Handbook of Liquid Crystals* Vol. 1 (Eds D Demus, J W Goodby, G W Gray, H-W Spiess, V Vill) (Weinheim: Wiley-VCH, 1998) p. 582
10. S Miyajima *EMIS Datarev. Ser.* **25** 457 (2000)
11. I Furó, S V Dvinskikh *Magn. Reson. Chem.* **40** S3 (2002)
12. M E Glicksman *Diffusion in Solids: Field Theory, Solid-State Principles and Applications* (New York: Wiley, 1999)
13. J W Emsley *Nuclear Magnetic Resonance of Liquid Crystals* (Dordrecht: Reidel, 1985)
14. J K Moscicki, Y-K Shin, J H Freed *J. Chem. Phys.* **99** 634 (1993)
15. M Iwahashi, Y Yamaguchi, T Kato, T Horiuchi, I Sakurai, M Suzuki *J. Phys. Chem.* **95** 445 (1991)
16. A Nayeem, S B Rananavare, V S S Sastry, J H Freed *J. Chem. Phys.* **91** 6887 (1989)
17. K Otnes, R Pynn, J A Janik, J M Janik *Phys. Lett. A* **38** 335 (1972)
18. J Topler, B Alefeld, T Springer *Mol. Cryst. Liq. Cryst.* **26** 297 (1974)

19. A J Leadbetter, F P Temme, A Heidemann, W S Howells *Chem. Phys. Lett.* **34** 363 (1975)
20. A J Leadbetter, R M Richardson, B A Dasannacharya, W S Howells *Chem. Phys. Lett.* **39** 501 (1976)
21. M P Fontana, M Ricco, C J Carlile, B Rosi-Schwartz *Physica B* **180–181** 726 (1992)
22. M P Fontana, G Gallone *Phys. Scr.* **T57** 168 (1995)
23. M Ricco, M P Fontana, B Rosi, C Vignali, M Cavazza *Mol. Cryst. Liq. Cryst.* **212** 139 (1992)
24. M Bee, A J Dianoux, J A Janik, J M Janik, R Podsiadly *Liq. Cryst.* **10** 199 (1991)
25. A J Dianoux, A Heidemann, F Volino, H Hervet *Mol. Phys.* **32** 1521 (1976)
26. A V Belushkin, M J Cook, D Frezzato, S D Haslam, A Ferrarini, D Martin, J McMurdo, P L Nordio, R M Richardson, A Stafford *Mol. Phys.* **93** 593 (1998)
27. M Hara, S Ichikawa, H Takezoe, A Fukuda *Jpn. J. Appl. Phys.* **23** 1420 (1984)
28. M Hara, H Tenmei, S Ichikawa, H Takezoe, A Fukuda *Jpn. J. Appl. Phys.* **24** L777 (1985)
29. M Hara, H Takezoe, A Fukuda *Jpn. J. Appl. Phys.* **25** 1756 (1986)
30. H Takezoe, M Hara, S Ichikawa, A Fukuda *Mol. Cryst. Liq. Cryst.* **122** 169 (1985)
31. T Nishikawa, J Minabe, H Takezoe, A Fukuda *Mol. Cryst. Liq. Cryst.* **231** 153 (1993)
32. T Moriyama, Y Takanishi, K Ishikawa, H Takezoe, A Fukuda *Liq. Cryst.* **18** 639 (1995)
33. W Urbach, H Hervet, F Rondelez *J. Chem. Phys.* **83** 1877 (1985)
34. H Hervet, W Urbach, F Rondelez *J. Chem. Phys.* **68** 2725 (1978)
35. D R Spiegel, A L Thompson, W C Campbell *J. Chem. Phys.* **114** 3842 (2001)
36. H Hakemi *J. Chem. Phys.* **79** 1434 (1983)
37. H Hakemi *Phys. Lett. A* **95** 35 (1983)
38. M Daoud, M Gharbia, A Gharbi *J. Phys. II* **4** 989 (1994)
39. M Daoud, G Louis, X Quelin, M Gharbia, A Gharbi, P Peretti *Liq. Cryst.* **19** 833 (1995)
40. M Daoud, M Gharbia, A Gharbi, C Destrade *Surf. Sci.* **349** L174 (1996)
41. M Daoud, K Rais, M Gharbia, A Gharbi, H T Nguyen *Braz. J. Phys.* **28** 284 (1998)
42. K Rais, M Gharbia, A Gharbi, H T Nguyen, C Destrade, M Daoud *Liq. Cryst.* **26** 1079 (1999)
43. A G Chmielewski *Mol. Cryst. Liq. Cryst.* **212** 205 (1992)
44. A V Chadwick, M Paykary *Mol. Phys.* **39** 637 (1980)
45. C K Yun, A G Fredrickson *Mol. Cryst. Liq. Cryst.* **12** 73 (1970)
46. F Noack, S Becker, J Struppe *Annu. Rep. NMR Spectrosc.* **33** 1 (1997)
47. M Vilfan, T Apih, A Gregorovic, B Zalar, G Lahajnar, S Zumer, G Hinze, R Böhmer, G Althoff *Magn. Reson. Imaging* **19** 433 (2001)
48. S V Dvinskikh, I Furó *J. Magn. Reson.* **146** 283 (2000)
49. S V Dvinskikh, I Furó *J. Magn. Reson.* **144** 142 (2000)
50. S V Dvinskikh, R Sitnikov, I Furó *J. Magn. Reson.* **142** 102 (2000)
51. S V Dvinskikh, I Furó *J. Magn. Reson.* **148** 73 (2001)
52. S V Dvinskikh, I Furó *J. Chem. Phys.* **115** 1946 (2001)
53. S V Dvinskikh, I Furó, D Sandström, A Maliniak, H Zimmermann *J. Magn. Reson.* **153** 83 (2001)
54. S V Dvinskikh, I Furó, H Zimmermann, A Maliniak *Phys. Rev. E* **65** 050702 (2002)
55. S V Dvinskikh, I Furó, H Zimmermann, A Maliniak *Phys. Rev. E* **65** 061701 (2002)
56. O Oishi, S Miyajima *J. Magn. Reson.* **160** 74 (2003)
57. O Oishi, S Miyajima *J. Phys. Soc. Jpn.* **71** 2373 (2002)
58. O Oishi, S Miyajima *J. Magn. Reson., Ser. A* **123** 64 (1996)
59. M Cifelli, C A Veracini *Phys. Chem. Chem. Phys.* **7** 3412 (2005)
60. M Cifelli, P J McDonald, C A Veracini *Phys. Chem. Chem. Phys.* **6** 4701 (2004)
61. J Kärger, H Pfeifer, W Heink *Adv. Magn. Reson.* **12** 1 (1988)
62. E O Stejskal, J E Tanner *J. Chem. Phys.* **42** 288 (1965)
63. J E Tanner *J. Chem. Phys.* **52** 2523 (1970)
64. P Stilbs *Prog. Nucl. Magn. Reson. Spectrosc.* **19** 1 (1987)
65. P T Callaghan *Principles of Nuclear Magnetic Resonance Microscopy* (Oxford: Oxford University Press, 1991)
66. W S Price *Conc. Magn. Reson.* **9** 299 (1997)
67. W S Price *Conc. Magn. Reson.* **10** 197 (1998)
68. E L Hahn *Phys. Rev.* **80** 580 (1950)
69. E O Stejskal *J. Chem. Phys.* **43** 3597 (1965)
70. G Lindblom, G Orädd *Prog. Nucl. Magn. Reson. Spectrosc.* **26** 483 (1994)
71. K Schmidt-Rohr, H W Spiess *Multidimensional Solid-State NMR and Polymers* (London: Academic Press, 1994)
72. G J Krüger, H Spiesecke *Z. Naturforsch. A* **28** 964 (1973)
73. G J Krüger, H Spiesecke, R V Steenwinkel, F Noack *Mol. Cryst. Liq. Cryst.* **40** 103 (1977)
74. G J Krüger, R Weiss *J. Phys. (France)*, **38** 353 (1977)
75. R Blinc, J Pirs, I Zupancic *Phys. Rev. Lett.* **30** 546 (1973)
76. R Blinc, M Burgar, M Luzar, J Pirs, I Zupancic, S Zumer *Phys. Rev. Lett.* **33** 1192 (1974)
77. I Zupancic, J Pirs, M Luzar, R Blinc, J W Doane *Solid State Commun.* **15** 227 (1974)
78. P Holstein, M Bender, P Galvosas, D Geschke, J Kärger *J. Magn. Reson.* **143** 427 (2000)
79. G J Krüger, H Spiesecke, R Weiss *Phys. Lett. A* **51** 295 (1975)
80. G J Krüger, H Spiesecke, R V Steenwinkel *J. Phys. Colloq. (France)* **37** C3 123 (1976)
81. S Miyajima, A F McDowell, R M Cotts *Chem. Phys. Lett.* **212** 277 (1993)
82. F Noack *Mol. Cryst. Liq. Cryst.* **113** 247 (1984)
83. M J Kim, K Cardwell, A K Khitrin *J. Chem. Phys.* **120** 11327 (2004)
84. J F Martin, L S Selwyn, R R Vold, R L Vold *J. Chem. Phys.* **76** 2632 (1982)
85. D Zax, A Pines *J. Chem. Phys.* **78** 6333 (1983)
86. J A Murphy, J W Doane *Mol. Cryst. Liq. Cryst.* **13** 93 (1971)
87. M E Moseley, A Loewenstein *Mol. Cryst. Liq. Cryst.* **90** 117 (1982)
88. V Breternitz, H Kresse *Phys. Lett. A* **54** 148 (1975)
89. A Pampel, J Kärger, D Michel *Chem. Phys. Lett.* **379** 555 (2003)
90. P T Callaghan, M A Le Gros, D N Pinder *J. Chem. Phys.* **79** 6372 (1983)
91. H Jóhannesson, I Furó, B Halle *Phys. Rev. E* **53** 4904 (1996)
92. R Y Dong, M Wiszniewska, E Tomchuk, E Bock *Solid State Commun.* **14** 691 (1974)
93. N Boden, L D Clark, C G Clarke, P K Kahol *Mol. Phys.* **50** 667 (1983)
94. R M Richardson, A J Leadbetter, D H Bonsor, G J Krüger *Mol. Phys.* **40** 741 (1980)
95. U Haberlen *High-Resolution NMR in Solids* (New York: Academic Press, 1976)
96. J Stepisnik *Physica B+C* **104** 350 (1981)
97. W-K Rhim, A Pines, J S Waugh *Phys. Rev. B* **3** 684 (1971)
98. W Zhang, D G Cory *Phys. Rev. Lett.* **80** 1324 (1998)
99. R Kimmich, J Niess, S Hafner *Chem. Phys. Lett.* **190** 503 (1992)
100. M Zhou, L Frydman *Solid State Nucl. Magn. Reson.* **4** 301 (1995)
101. I Chang, G Hinze, G Diezemann, F Fujara, H Sillescu *Phys. Rev. Lett.* **76** 2523 (1996)
102. L Werbelow, G Pouzard *J. Phys. Chem.* **85** 3887 (1981)
103. J Kärger, N K Bar, W Heink, H Pfeifer, G Seiffert *Z. Naturforsch., A* **50** 186 (1995)
104. P Galvosas, F Stallmach, G Seiffert, J Kärger, U Kaess, G Majer *J. Magn. Reson.* **151** 260 (2001)
105. P T Callaghan, M E Komlosh, M Nyden *J. Magn. Reson.* **133** 177 (1998)
106. N V Kashirin, V D Skirda, I V Ovchinnikov *Kolloid. Zh.* **62** 78 (2000) [a]
107. A V Filippov, V D Skirda *Kolloid. Zh.* **62** 837 (2000) [a]
108. A V Uryadov, V D Skirda *Kolloid. Zh.* **63** 259 (2001) [a]
109. R R Valiullin, V D Skirda, S Stapf, R Kimmich *Phys. Rev. E* **55** 2664 (1997)
110. N L Zakhartchenko, V D Skirda, R R Valiullin *Magn. Reson. Imaging* **16** 583 (1998)
111. V D Skirda, I Y Aslanyan, O E Philippova, N S Karybiants, A R Khokhlov *Macromol. Chem. Phys.* **200** 2152 (1999)
112. R Kimmich, W Unrath, G Schnur, E Rommel *J. Magn. Reson.* **91** 136 (1991)
113. B Geil *Conc. Magn. Reson.* **10** 299 (1998)
114. M Cifelli, V Domenici, C A Veracini *Mol. Cryst. Liq. Cryst.* **429** 167 (2005)

115. A K Khitrin, V L Ermakov, B M Fung *Chem. Phys. Lett.* **360** 161 (2002)
116. F Noack *Prog. Nucl. Magn. Reson. Spectrosc.* **18** 171 (1986)
117. F Noack, M Notter, W Weiss *Liq. Cryst.* **3** 907 (1988)
118. D Pusiol, F Noack *Liq. Cryst.* **5** 377 (1989)
119. R Köllner, K H Schweikert, F Noack, H Zimmermann *Liq. Cryst.* **13** 483 (1993)
120. P J Sebastiao, A C Ribeiro, H T Nguyen, F Noack *Z. Naturforsch., A* **48** 851 (1993)
121. J Struppe, F Noack *Liq. Cryst.* **20** 595 (1996)
122. S V Dvinskikh, Yu V Molchanov, A L Gorid *Vestn. Lening. Univ., Ser. 4* **3** 15 (1989)
123. M V Terekhov, S V Dvinskikh, A F Privalov *Appl. Magn. Reson.* **15** 363 (1998)
124. H C Torrey *Phys. Rev.* **92** 962 (1953)
125. S Zumer, M Vilfan *Phys. Rev. A* **17** 424 (1978)
126. S Zumer, M Vilfan *J. Mol. Struct.* **46** 475 (1978)
127. M Vilfan, S Zumer *Phys. Rev. A* **21** 672 (1980)
128. R Stannarius, S Oehler, H Schmiedel *Mol. Cryst. Liq. Cryst.* **192** 209 (1990)
129. R Stannarius, H Schmiedel *Liq. Cryst.* **5** 389 (1989)
130. R Stannarius, H Schmiedel *J. Magn. Reson.* **81** 339 (1989)
131. S Oehler, R Stannarius, H Schmiedel *Z. Naturforsch., A* **43** 687 (1988)
132. R Stannarius, H Schmiedel *J. Magn. Reson.* **65** 1 (1985)
133. M Luzar, B Lozar, R Blinc, J W Doane *Mol. Cryst. Liq. Cryst.* **113** 291 (1984)
134. Z Yaniv, G Chidichimo, N Vaz, J W Doane *Phys. Lett. A* **86** 297 (1981)
135. N A P Vaz, G Chidichimo, Z Yaniv, J W Doane *Phys. Rev. A* **26** 637 (1982)
136. G Chidichimo, Z Yaniv, N A P Vaz, J W Doane *Phys. Rev. A* **25** 1077 (1982)
137. B Zalar, A Gregorovic, R Blinc *Phys. Rev. E* **62** R37 (2000)
138. R R Ernst, D Bodenhausen, A Wokaun *Principles of Nuclear Magnetic Resonance in One and Two Dimensions* (Oxford: Clarendon Press, 1987)
139. I Furó, H Jóhannesson *J. Magn. Reson., Ser. A* **119** 15 (1996)
140. M Kadi, S V Dvinskikh, I Furó, M Almgren *Langmuir* **18** 5015 (2002)
141. P T Callaghan, O Soderman *J. Phys. Chem.* **87** 1737 (1983)
142. P T Callaghan, I Furó *J. Chem. Phys.* **120** 4032 (2004)
143. P T Callaghan, S Godefroy, B N Ryland *Magn. Reson. Imaging* **21** 243 (2003)
144. P T Callaghan, M E Komlosh *Magn. Reson. Chem.* **40** S15 (2002)
145. W Franklin *Phys. Rev. A* **11** 2156 (1975)
146. K-S Chu, D S Moroi *J. Phys. Colloq. (France)* **36** C1 99 (1975)
147. S Hess, D Frenkel, M P Allen *Mol. Phys.* **74** 765 (1991)
148. M P Allen *Phys. Rev. Lett.* **65** 2881 (1990)
149. P Ilg *Phys. Rev. E* **71** 051407 (2005)
150. F Volino, A J Dianoux *Mol. Phys.* **36** 389 (1978)
151. F Volino, A J Dianoux, A Heidemann *J. Phys. Lett. (France)* **40** L583 (1979)
152. G Moro, P L Nordio, U Segre *Chem. Phys. Lett.* **105** 440 (1984)
153. W L McMillan *Phys. Rev. A* **4** 1238 (1971)
154. K M Aoki, F Yonezawa *Phys. Rev. A* **46** 6541 (1992)
155. E de Miguel, L F Rull, K E Gubbins *Phys. Rev. A* **45** 3813 (1992)
156. S Sarman, D J Evans *J. Chem. Phys.* **99** 620 (1993)
157. C W Cross, B M Fung *J. Chem. Phys.* **101** 6839 (1994)
158. A V Komolkin, A Laaksonen, A Maliniak *J. Chem. Phys.* **101** 4103 (1994)
159. S Cozzini, L F Rull, G Ciccotti, G V Paolini *Physica A* **240** 173 (1997)
160. J S van Duijneveldt, M P Allen *Mol. Phys.* **92** 855 (1997)
161. I Cacelli, S Campanile, G Prampolini, A Tani *J. Chem. Phys.* **117** 448 (2002)
162. R L B Selinger *Phys. Rev. E* **65** 051702 (2002)
163. M A Bates, G R Luckhurst *J. Chem. Phys.* **120** 394 (2004)
164. G Cinacchi, L De Gaetani, A Tani *J. Chem. Phys.* **122** 184513 (2005)
165. G Cinacchi, R Colle, A Tani *J. Phys. Chem. B* **108** 7969 (2004)
166. R Blinc, V Dimic, J Pirs, M Vilfan, I Zupancic *Mol. Cryst. Liq. Cryst.* **14** 97 (1971)
167. S K Ghosh, E Tettamanti *Lett. Nuovo Cimento* **40** 197 (1984)
168. R Blinc, B Marin, J Pirs, J W Doane *Phys. Rev. Lett.* **54** 438 (1985)
169. M Vilfan, G Lahajnar, I Zupancic, S Zumer, R Blinc, G P Crawford, J W Doane *J. Chem. Phys.* **103** 8726 (1995)
170. S K Ghosh, E Tettamanti *Chem. Phys. Lett.* **69** 403 (1980)
171. R J Hayward, K J Packer *Mol. Phys.* **26** 1533 (1973)
172. L Miljkovic, T Thompson, M M Pintar, R Blinc, I Zupancic *Chem. Phys. Lett.* **38** 15 (1976)
173. G Rollmann, K F Reinhart, F Noack *Z. Naturforsch., A* **34** 964 (1979)
174. S K Ghosh, E Tettamanti, A Ricchiuto *Chem. Phys. Lett.* **101** 499 (1983)
175. E R Gasilova, V A Shevelev *Liq. Cryst.* **27** 579 (2000)
176. J Xu, C A Veracini, R Y Dong *Phys. Rev. E* **72** 051703 (2005)
177. S V Dvinskikh, D Sandström, H Zimmermann, A Maliniak *Prog. Nucl. Magn. Reson. Spectrosc.* **48** 85 (2006)
178. R Y Dong, D Goldfarb, M E Moseley, Z Luz, H Zimmermann *J. Phys. Chem.* **88** 3148 (1984)
179. I Ando, M Kobayashi, C Zhao, Y Yin, S Kuroki, in *Encyclopedia of Nuclear Magnetic Resonance* (Eds D M Grant, R K Harris) (Chichester: Wiley, 2002) p. 770
180. Y Yin, C Zhao, S Kuroki, I Ando *J. Chem. Phys.* **113** 7635 (2000)
181. Y Yin, C Zhao, S Kuroki, I Ando *Macromolecules* **35** 2335 (2002)
182. S Kanesaka, H Kimura, S Kuroki, I Ando, S Fujishige *Macromolecules* **37** 453 (2004)
183. G J Krüger, H Spiesecke *Ann. Phys.* **3** 193 (1978)
184. G J Krüger, H Spiesecke, R V Steenwinkel *J. Phys. Colloq. (France)* **36** C1 (1975)
185. M E Moseley *J. Phys. Chem.* **87** 18 (1983)
186. M E Moseley, A Loewenstein *Mol. Cryst. Liq. Cryst.* **95** 51 (1983)
187. M E Moseley, R Poupko, Z Luz *Mol. Cryst. Liq. Cryst.* **95** 279 (1983)
188. A Loewenstein *Chem. Phys. Lett.* **38** 543 (1976)
189. J A Murphy, J W Doane, Y Y Hsu, D L Fishel *Mol. Cryst. Liq. Cryst.* **22** 133 (1973)
190. H W Long, M Luzar, H C Gaede, R G Larsen, J Kritzenberger, A Pines, G P Crawford *J. Phys. Chem.* **99** 11989 (1995)
191. J Ruohonen, J Jokisaari *Phys. Chem. Chem. Phys.* **3** 3208 (2001)
192. J Ruohonen, M Ylihautala, J Jokisaari *Mol. Phys.* **99** 711 (2001)
193. M Cifelli, J Saunavaara, J Jokisaari, C A Veracini *J. Phys. Chem. A* **108** 3973 (2004)
194. J Jokisaari, in *NMR of Ordered Liquids* (Eds E E Burnell, C A de Lange) (Dordrecht: Kluwer Academic, 2003) p. 109

[a] — *Colloid. J. (Engl. Transl.)*